27
3-10-77
25 NTIS

SAND 76-0727
Unlimited Release

3151

FRACTURE MECHANICS OF OIL SHALE - SOME PRELIMINARY RESULTS

MASTER

R. A. Schmidt and C. W. Huddle

Prepared by Sandia Laboratories, Albuquerque, New Mexico 87115
and Livermore, California 94550 for the United States Energy Research
and Development Administration under Contract AT (29-1)-789

Printed February 1977

Sandia Laboratories

SF 2900 Q(7-73)

Issued by Sandia Laboratories, operated for the United States Energy Research & Development Administration by Sandia Corporation.

NOTICE

Printed in the United States of America
Available from
National Technical Information Service
U. S. Department of Commerce
5285 Port Royal Road
Springfield, VA 22161
Price: Printed Copy $ 4.00 ; Microfiche $3.00

DISCLAIMER

SAND 76-0727
Unlimited Release
Printed February 1977

FRACTURE MECHANICS OF OIL SHALE - SOME PRELIMINARY RESULTS

R. A. Schmidt and C. W. Huddle
Geomechanics Research Division
Sandia Laboratories
Albuquerque, New Mexico 87115

ABSTRACT

Results of a comprehensive series of fracture toughness tests on oil shale from Anvil Points are presented. Since oil shale is layered and transversely isotropic, three-point-bend specimens representing 20 and 40 gal/ton were tested in the three principal crack orientations - divider, arrester, and short transverse.

These specimens were fatigue cracked to produce a sharp natural crack in a stable manner by means of loading between fixed limits of the crack opening displacement. Crack front position was marked by immersing the specimen in a penetrating dye so that the crack length could be determined after final failure.

Load-to-failure records of load vs. crack opening displacement showed evidence of crack surface interference or crack closure. Fracture toughness was found to decrease by approximately 40 percent for an increase in kerogen content from 20 to 40 gal/ton. Highest values of fracture toughness were found for the divider geometry, lowest for short transverse, and intermediate for arrester with the actual values varying from 0.3 to 1.1 MN $m^{-3/2}$.

INTRODUCTION

Many failure criteria and theories such as the Mohr criterion exist that predict failure conditions for rock. However, these theories often deal only with competent rock and do not deal directly with fracture processes. As a result, they cannot be expected to deal with questions of crack propagation such as (1) the length of major crack extension in processes such as hydraulic fracturing, (2) failure loads necessary to extend pre-existing fractures as might be encountered in repeated borehole explosive tests, and (3) conditions for crack bifurcation or branching necessary to create rubble in a rock fragmentation process. These and similar problems are of obvious importance to the bed preparation techniques now being discussed and tested for in-situ oil shale retorting.

In the past 20 years, many investigations involving crack propagation in brittle metal alloys have employed the well-founded discipline of linear elastic fracture mechanics, LEFM, with great success. Although this theory is based on linear elasticity and is directly related to the Griffith theory [1], plastic flow and other nonlinear behavior can occur on a small scale without affecting its predictive success. Purely brittle behavior is not required and only when the size of the zone of nonlinear behavior at a crack tip cannot be considered small when compared to the crack length does recourse to more elaborate fracture theories such as the J integral [2] become necessary.

LEFM is based on the stress intensity factor, K, which quantifies the intensity of the stress singularity at a crack tip. Fracture mechanics states that a crack will advance when its stress intensity reaches a critical value, K_{Ic}, assuming that the crack tip is in a state of plane strain. This value of K_{Ic}, known as plane strain fracture toughness, has been shown to be a measurable material constant for a vast number of metal alloys, glasses, polymers, and even some organic materials such as wood, paper, and rubber.

Fracture mechanics is related to Griffith theory [1] which as modified by Orowan [3] and restated by Irwin [4] equates the critical rate of strain energy release during crack extension, G_{Ic}, to twice the effective surface energy.

$$G_{Ic} = 2\gamma_{eff}$$

The effective surface energy is considered to include dissipative energy processes such as plastic flow and microcracking. Several rock mechanics investigations [5-7] have sought to measure γ_{eff} directly. Difficulties arise, even if plastic flow can be neglected, when attempts are made to estimate the total surface area created in crack propagation. On the other hand, the fracture mechanics approach has simply been to measure the value of the other side of the equation, the critical strain energy release rate, G_{Ic}, by using a specimen with known crack geometry. G_{Ic} is directly related to K_{Ic} by the following equation:

$$G_{Ic} = \frac{(1 - \nu^2)}{E} K_{Ic}^2$$

where ν is Poisson's ratio and E is Young's modulus.

Recent investigations have measured the fracture toughness, K_{Ic}, of several rocks [8-12]. These reported values should probably be considered preliminary or apparent fracture toughness, K_Q, since specimen size requirements set by ASTM for toughness testing of metallic materials [ASTM Designation: E399-72T] were not completely fulfilled. No standards have, as yet, been set for fracture toughness tests of rock, but Schmidt [9] has indicated that the present standards for metals appear to be applicable, at least for one rock, Indiana limestone. In fact, the apparent fracture toughness of Indiana limestone is subject to effects of specimen size in a manner typical of aluminum alloys [9]. In addition, fracture tests performed on specimens of Indiana limestone loaded in a pressure vessel have shown that moderate confining pressures can cause a substantial increase in the fracture toughness of this material [12].

This laboratory is currently investigating the fracture behavior of oil shale and, specifically, measuring the fracture toughness of this material. In addition, the effects of confining pressure and environmental factors on fracture toughness are to be assessed. This report in particular contains information that deals with a comprehensive set of unconfined fracture toughness tests performed on two grades of oil shale on specimens 2.5 x 5 x 20 cm (1 x 2 x 8 in) in size and oriented in the three principal crack geometries.

SPECIMEN PREPARATION

Two large blocks of oil shale (B2 and D2), obtained from the Anvil Points mine near Rifle, Colorado, were selected as material for specimens. These blocks had been previously cored and characterized as to their kerogen content by nuclear magnetic resonance (NMR) and density. They were also used for obtaining samples for triaxial compression tests in a companion study and represent, nominally, 20 and 40 gal/ton kerogen. The portions of the blocks used in this study were selected on the basis of competent unfractured material, consistent grade as determined from NMR analysis, and visual homogeneity. Areas containing lenses and other impurities were excluded.

The two large blocks were first cut into slabs 13 cm (5 in) thick using a wire saw. Standard three-point-bend fracture specimens were then rough machined with a band saw and finished by grinding. Specimens were prepared in the three principal crack geometries - arrester, divider, and short transverse - as depicted in Fig. 1. Some difficulty was encountered in obtaining sufficient competent material for short transverse specimens since its longest dimension is perpendicular to the bedding planes and a majority of the flaws and cracks were found to lie in the bedding planes.

EXPERIMENTAL TECHNIQUES

A 980 kN (220 kip) servo-controlled MTS* load frame was used for both fatigue cracking and final fracture. The specimen loading configuration is shown in Fig. 2. In order to obtain stability during fatigue cracking and during the final load-to-failure, loading was performed by controlling the crack opening displacement, i.e. displacement across the notch. The necessary sensitivity for this displacement measurement was obtained using an LVDT displacement transducer having a linear range of ± 0.25 mm (± 0.010 in). Displacements were measured and controlled accurately to better than 20 nm (1 microinch).

A single fatigue crack was made to propagate from the machined notch by repeated loading to approximately 85 percent of the fracture load. This loading was actually performed by a sinusoidal variation of crack opening displacement. By controlling displacement, the load automatically decreases as the crack grows providing the stability needed to fatigue crack this brittle material.

*MTS Systems Corp., Minneapolis, Minn.

In previous investigations [9] the average length of the fatigue crack was measured indirectly by comparing the specimen's compliance (inverse slope of load-displacement record) with a compliance calibration. The compliance calibration is made by measuring the compliance of a similar specimen in which a sharp notch of known length is cut into the specimen. This process is repeated several times with successively deeper notches. However, this procedure was deemed impractical for the oil shale investigation since compliance calibrations would have to be performed for each crack geometry and for both grades of shale. Also, material inhomogeneity would make the accuracy of the results somewhat uncertain.

Instead, the position of the fatigue crack was marked by immersing the specimen in a fluorescent dye penetrant called Zyglo* after fatigue cracking was complete. After the final load-to-failure the specimen was then broken in half, making the marked crack front visible (Figs. 3, 4). The average length of the fatigue crack was then determined by digitizing the position of the crack front from a photograph of the fracture surface and by computer reduction of this digitized data.

Additional tests were performed to determine if the presence of penetrating dye in the crack could affect the final results. Specimens were selected that closely matched the specimens that had been tested using Zyglo. Each specimen was fatigue cracked until the same level of compliance was achieved as in its companion test. Hence, the average crack length could be assumed to be the same in both tests before the final load-to-failure. The validity of this assumption of equal crack lengths was verified by direct measurement as discussed in the next section.

---

*Registered trademark of Magnaflux Corp., Chicago, IL.

RESULTS AND DISCUSSION

Photographs of fracture surfaces from specimens that were immersed in Zyglo after fatigue cracking are shown in Figs. 3, 4. Unlike fractures in Charcoal granite [8], the Zyglo was found to stain the fatigue crack surface sufficiently well to distinguish the crack front without necessitating the use of ultraviolet light. Fig. 3 shows "well-behaved" fatigue cracks for specimens in all three crack orientations. Occasional difficulty was encountered in producing uniform fatigue cracks, particularly in the short transverse orientation. Fig. 4 shows an example of how a fatigue crack in a short transverse specimen was drawn into a weak bedding plane that contained a flaw. Since a measure of the average crack length would be meaningless for these cases, such test results were discarded.

Fig. 5 is a photograph of a fracture surface that was not marked with Zyglo. Notice, however, that the regions of fatigue cracking, load-to-failure, and final separation* are distinguishable. This change in appearance of the fracture surface had not been observed for the previous fracture tests on other rocks. The crack front location of the fatigue precrack was digitized and an average crack length calculated. This value was found to differ by only 0.6 percent from the assumed value as deduced from a similar specimen precracked to the same compliance and immersed in Zyglo. The fracture surface of Fig. 5 was examined using a scanning electron microscope, however no difference in detailed features was observed.

Typical load vs. crack-opening-displacement records at various stages of fatigue cracking are shown in Fig. 6. The general trends of these records are the same as for the two previously tested rocks, Indiana lime-

*Final separation was accomplished by simply breaking the specimen in half manually.

stone [9] and charcoal granite [8]. Before any crack is advanced the load cycle is nearly linear elastic. As cracking begins the initial loading is nonlinear becoming linear at moderate loads but nearly all displacement is recoverable. The change from nonlinear to linear behavior indicates that crack surface interference, sometimes called crack closure, is occurring in which the crack surfaces do not fit together perfectly and, hence, contact each other upon unloading before zero load is reached [9,13]. The slopes of all the curves near zero load are approximately equal to the slope of the first loading cycle when there was no crack. This means that the crack is tightly closed at zero load such that the initial loading takes place as if there were no crack present.

Since the machined notches on all specimens were of the same length, the slope of the first loading cycle can be correlated with Young's modulus. The slopes, although not significant in themselves, correlate very well with the modulus values obtained from the unconfined uniaxial compression tests on oil shale from the same blocks. Note that the initial slope of records for the short transverse geometry would compare to the compression tests in which stress is perpendicular to the bedding planes. The arrester and divider geometries correlate with tests parallel to bedding.

The final load-to-failure was performed in each test by slowly increasing the crack opening displacement, COD, at a constant rate of 0.84 μm/s (33 μ in/s). The typical load vs COD record of Fig. 7 shows the initial nonlinearity as the crack opens, a linear portion where the crack is fully open, followed by further nonlinearity as the crack tip zone of microcracking expands, and finally stable crack growth as the load drops.

Anomalous results were obtained, however, for two specimens from block D (40 gal/ton) and tested in the arrester geometry which produced load vs COD records that were rather nonlinear throughout and, consequently, values of fracture toughness from these tests are of questionable accuracy.

Anomalous results were also obtained in the arrester geometry for specimens of block B (20 gal/ton) as typified by Fig. 8. While this record shows a linear portion, the crack growth was not completely stable. Sharp load drops occurred which were accompanied by audible crack bursts. Also, load increases occurred when the crack was seen to begin propagating in the bedding planes causing crack tip blunting and delamination. These sizable and audible crack bursts, while not unexpected for this geometry, have not been previously observed, to our knowledge, on tests such as these. The existence of audible crack bursts may have some significance for the detection of crack growth during quasi-static hydraulic fracturing.

Preliminary values of fracture toughness are calculated from crack length and load at "failure" [14]. Crack length determination was previously discussed. The "failure" load, P_Q, which is that load corresponding to an "effective" crack extension of 2 percent, is determined by the intersection of the load vs. COD record with a secant line of the required slope [15] (Fig. 7). The resulting value of fracture toughness is considered preliminary since tests on larger samples have not, as yet, been performed to determine if the limiting value, K_{Ic}, has been adequately evaluated. Tensile strengths will also need to be determined from "direct pull" tests.

Values of preliminary fracture toughness are presented in Fig. 9. Tests that were performed in pairs show that there is little or no effect of the Zyglo immersion on toughness. Also scatter between pairs of tests is remarkably small considering the variability of oil shale and the fact that scatter in fracture toughness of metal alloys is often 10 percent or more.

By comparing results among tests of similar kerogen content, fracture toughness is seen to be highest for the divider geometry and lowest for the short transverse with the arrester results being intermediate. The fact that the values for short transverse are lowest is not surprising if the bedding planes are considered planes of weakness, but one might expect arrester results to be highest. Man-made composites made of plates of different materials are typically tougher in the arrester orientation as a result of crack tip blunting at material interfaces. Oil shale is not, however, simply made up of two discrete materials and the material properties of the various layers do not differ as much as those of typical composites.

Fracture toughness of material from block B with 20 gal/ton is seen to be consistently higher (by about 40 percent) than block D (40 gal/ton) suggesting that fracture toughness decreases with an increase in kerogen content. This result was also somewhat unexpected since uniaxial compression tests on Anvil Points oil shale had previously shown little change in compressive strength for an increase in kerogen content from 16 to 41 gal/ton [16]. However, recent compression tests on material from the same blocks that were used for the toughness tests do show a 33 percent decrease in strength for an increase in kerogen content from 20 to 40 gal/ton. On the other hand, since these compression tests indicated a large increase in the "failure" strain for an increase in kerogen content, one might deduce that more energy is required to fracture the richer material implying an increase in fracture toughness. But substantial crack growth and dilatancy are known to occur in compression tests of rock long before maximum stress or "failure" strain is reached. If the stress at maximum volume strain is assumed to correspond to a point of significant crack growth, then it is reasonable to use the axial strains at this stress level rather than the "failure" strain in a comparison of the relative fracture energies. In the recent compression tests, little difference was noted between values of the axial strain corresponding to maximum volume strain for the 20 and 40 gal/ton shale, implying that the reasonably good correlation of simple compressive strengths to fracture toughness should not be entirely unexpected. Comparison of tensile properties with toughness may prove to be more appropriate and will be correlated when the tension test results are available.

Although the fracture specimens were taken from blocks of oil shale that were nominally 20 and 40 gal/ton, it is important to obtain the actual kerogen content of specimens tested and the extent of variability within each specimen. Small cores can be removed from each specimen that was tested successfully, and nuclear magnetic resonance analysis of these cores will be included in a future report.

SUMMARY

1) Three-point-bend fracture toughness specimens of oil shale from the Anvil Points mine representing 20 and 40 gal/ton were machined in three orientations -- divider, arrester, and short transverse.
2) These specimens were fatigue precracked in a servo-controlled MTS load frame using a sinusoidal variation of the crack opening displacement as measured by a short range LVDT.

3) Crack lengths were determined after fatigue cracking by immersing the specimens in a fluorescent dye penetrant, marking the fracture surface so that the average crack length could be determined after the specimen was broken in half.

4) Specimens were loaded to failure using the same configuration as for fatigue cracking.

5) Load vs crack opening displacement records showed evidence of crack surface interference or crack closure.

6) Final crack growth was stable except for tests of 20 gal/ton in the arrester geometry for which audible crack bursts were detected.

7) Fracture toughness was found to decrease by approximately 40 percent for an increase in kerogen content from 20 to 40 gal/ton.

8) Highest values of fracture toughness were found for the divider geometry, lowest for short transverse, and intermediate for arrester.

9) Fracture toughness varied from 0.3 to 1.1 MN $m^{-3/2}$ with little scatter of results.

10) Compliance and fracture toughness obtained in the present fracture tests were found to correlate well with Young's modulus and compressive strength, respectively, obtained from earlier uniaxial compression tests on similar material.

REFERENCES

1) Griffith, A. A., "The Theory of Rupture," Proc. of First Int'l. Cong. Appl. Mech., 55 (1924).

2) Rice, J. R., "A Path Independent Integral and the Approximate Analysis of Strain Concentration by Notches and Cracks," J. of App. Mech., 35, 379 (1968).

3) Orowan, E., Fatigue and Fracture of Metals, Proc. of 1950 Conf. at M.I.T., John Wiley, N.Y., 139 (1952).

4) Irwin, G. R., "Analysis of Stresses and Strains Near the End of a Crack Traversing a Plate," J. of App. Mech., 24, 361 (1957).

5) Gilman, J. J., "Direct Measurements of the Surface Energy of Crystals," J. Appl. Phys., 31, 2208-2218 (1960).

6) Perkins, T. K., and Krech, W. W., "Effect of Cleavage Rate and Stress Level on Apparent Surface Energies of Rocks," Soc. Petrol. Engrs. J., 6, 4, 308-314 (1966).

7) Friedman, M., Handin, J., and Alani, G., "Fracture Surface Energy of Rocks," Int. J. Rock Mech. Min. Sci., 9, 757-766 (1972).

8) Schmidt, R. A., "Fracture Toughness of Rock Materials with Application to In Situ Fragmentation of Oil Shale Beds," presented at the Symposium on Alternate Fuel Resources, Am. Inst. of Aeronautics and Astronautics, Santa Maria, Calif. (1976).

9) Schmidt, R. A., "Fracture-Toughness Testing of Limestone," Exp. Mech., 16, 5, 161-167 (1976).

10) Clifton, R. J., Simonson, E. R., Jones, A. H., and Green, S. J., "Determination of the Critical Stress Intensity Factor K_{Ic} from Internally-Pressurized Thick-Walled Vessels," Exp. Mech., 16, 6, 233-238 (1976).

11) Barker, L. M., "A Simplified Method for Measuring Plane Strain Fracture Toughness," submitted to Engineering Fracture Mechanics (1976).

12) Schmidt, R. A., and Huddle, C. W., "Effect of Confining Pressure on Fracture Toughness of Indiana Limestone," preprint-proceedings of 17th U.S. Symposium on Rock Mechanics, 1976.

13) Elber, W., "The Significance of Fatigue Crack Closure," Damage Tolerance in Aircraft Structures, ASTM STP 486, 230 (1971).

14) American Society for Testing and Materials, "Tentative Method of Test for Plane Strain Fracture Toughness of Metallic Materials (ASTM Designation: E399-72T)," 1972 Annual Book of Standards, Part 31, ASTM, Phila. (1972).

15) Brown, W. F., and Srawley, J. E., "Plane Strain Crack Toughness Testing of High Strength Metallic Materials," ASTM STP 410, ASTM, 1-65 (1966).

16) Schmidt, R. A., and Schuler, K. W., "Mechanical Properties of Oil Shale from Anvil Point under Conditions of Uniaxial Compression," Sandia Laboratories Report SAND-74-0035, August, 1974.

GEOMETRIES

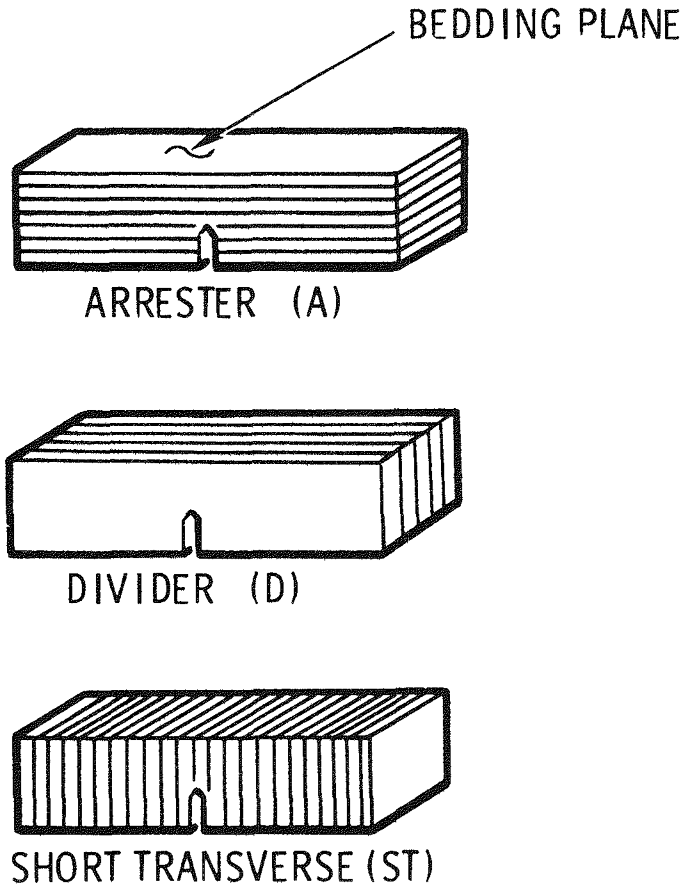

Fig. 1 Illustration of the principal crack orientations with respect to bedding planes.

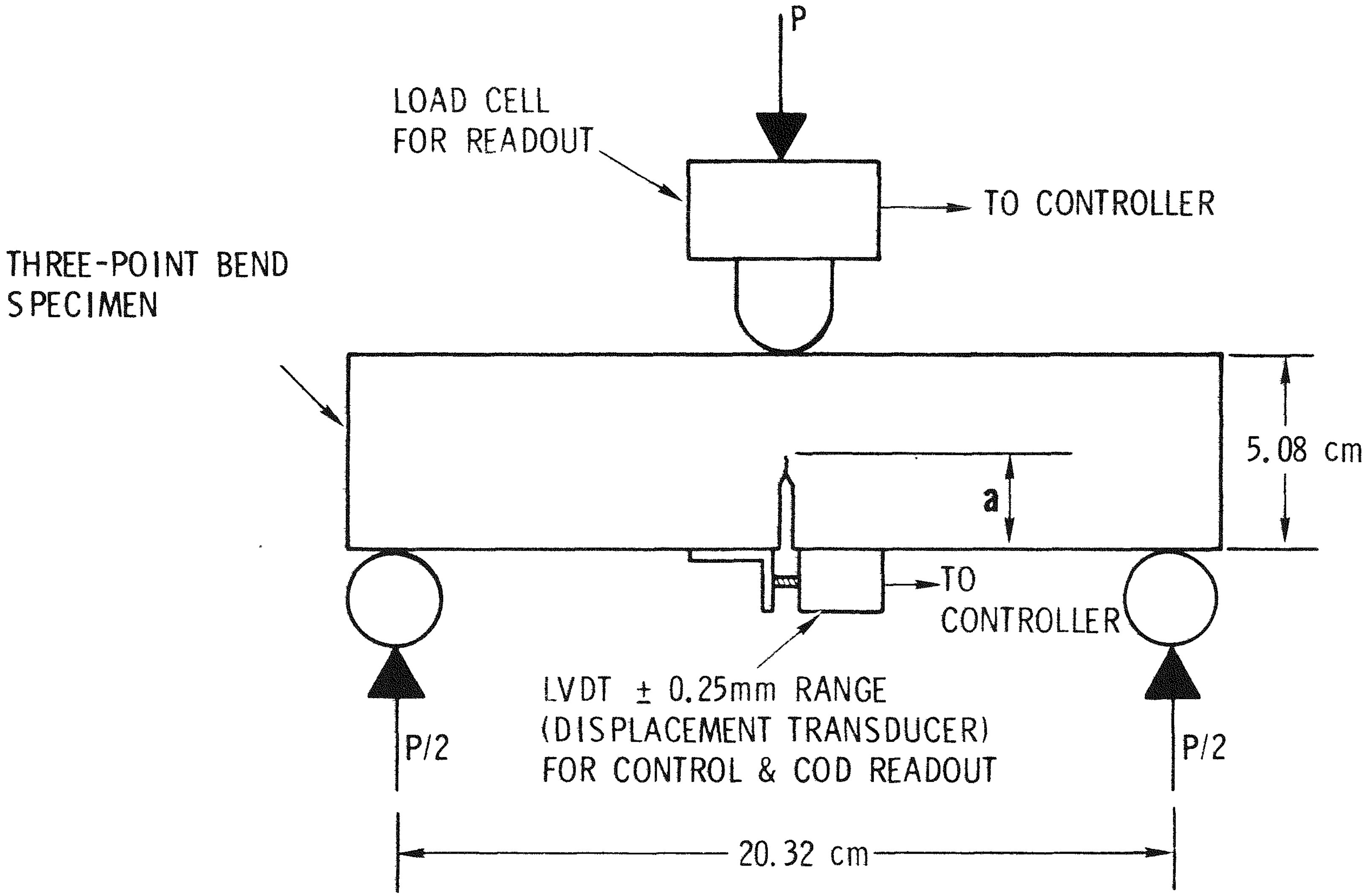

Fig. 2 Three-point-bend test configuration.

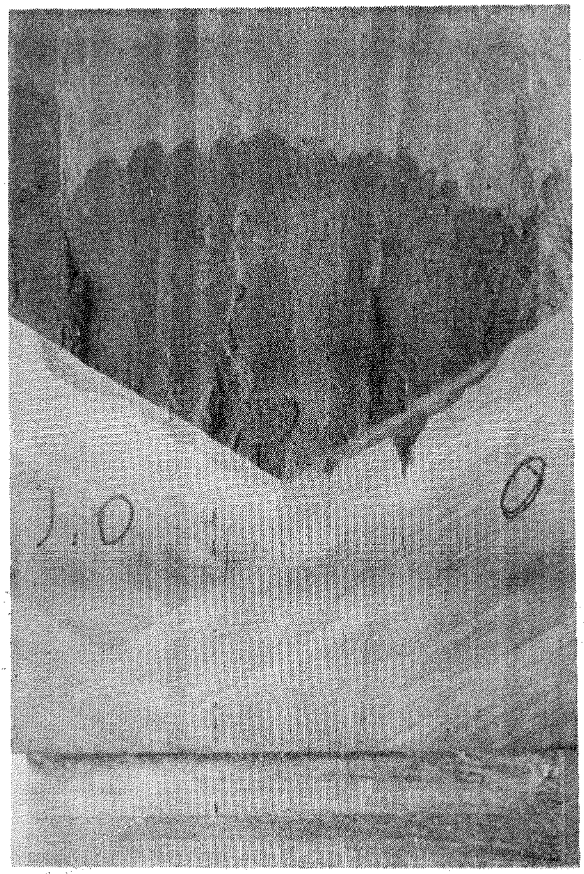

Fig. 3a Fatigue crack surface marked with Zyglo in divider geometry.

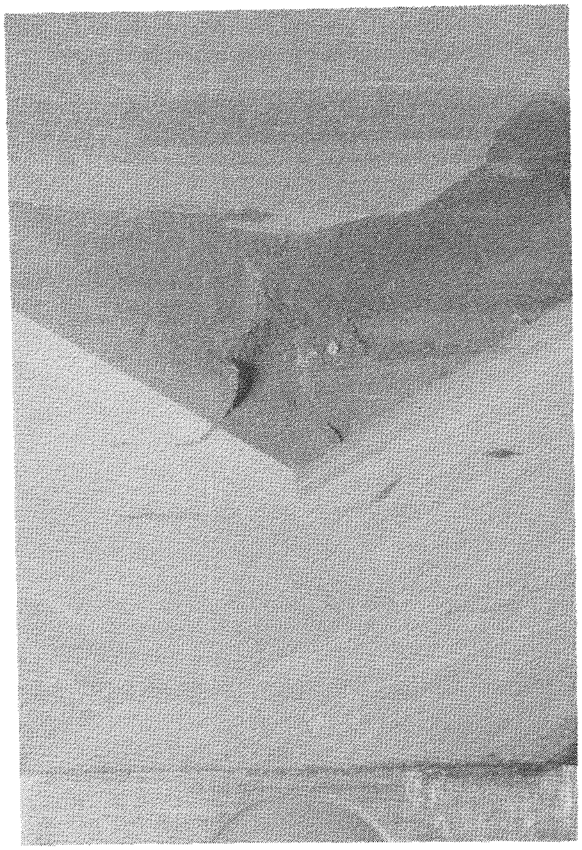

Fig. 3b Fatigue crack surface marked with Zyglo in arrester geometry.

Fig. 3c Fatigue crack surface marked with Zyglo in short transverse geometry.

Fig. 4 Fatigue crack surface marked with Zyglo for short transverse specimen showing unacceptable crack front shape caused by preexisting flaw.

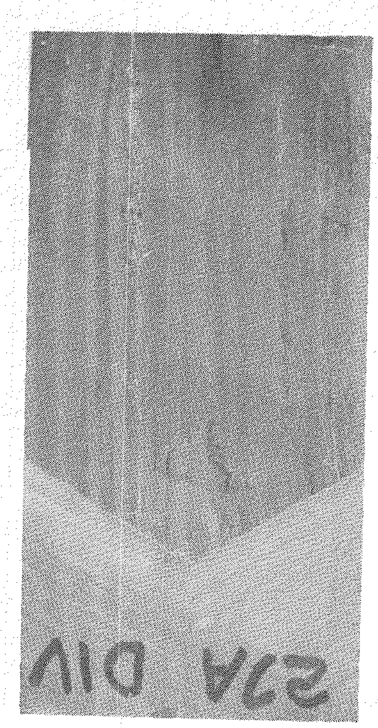

Fig. 5 Fatigue crack surface not marked with Zyglo in divider geometry.

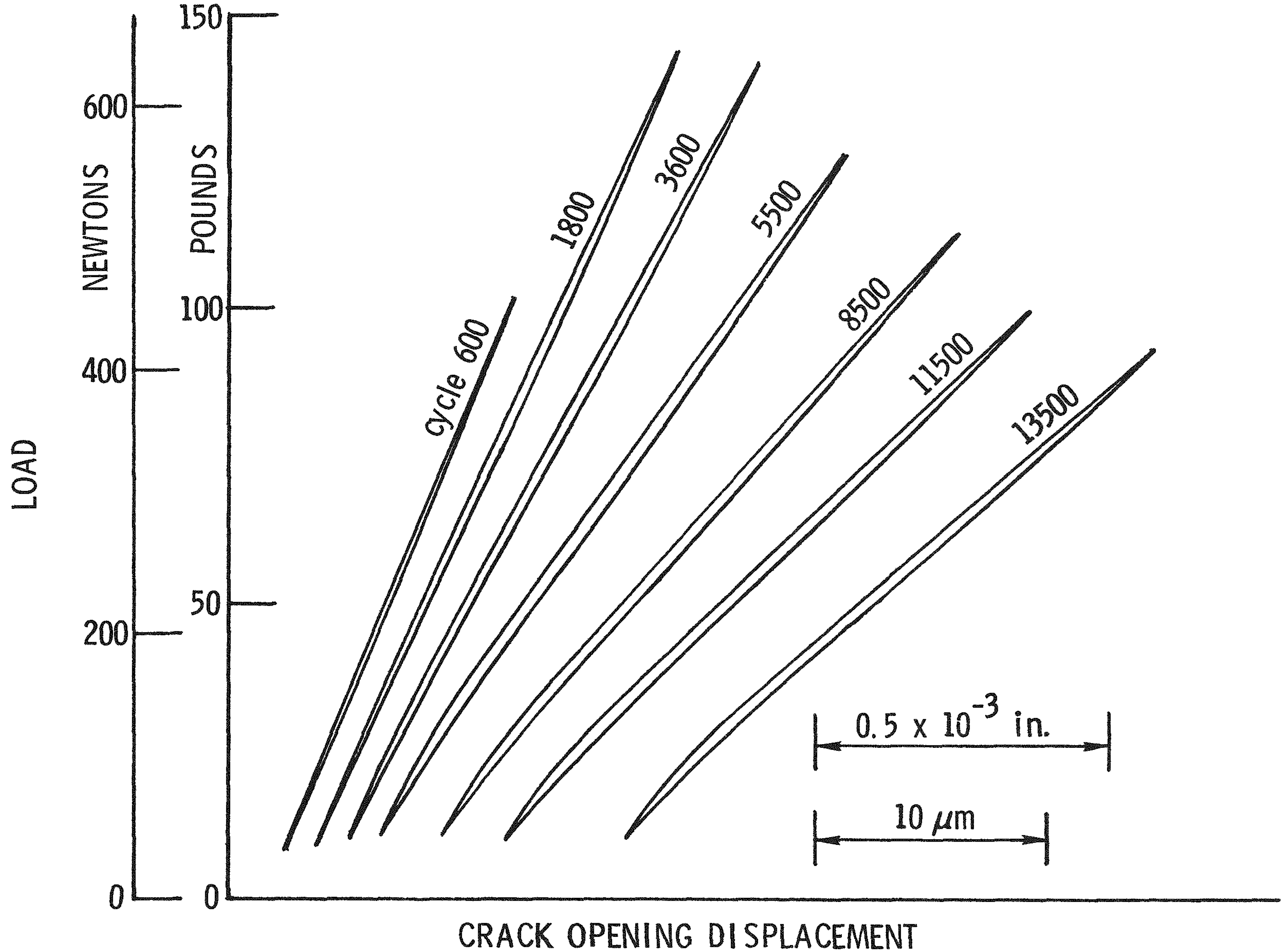

Fig. 6 Load vs. COD for various cycles of fatigue precracking for oil shale fracture specimen.

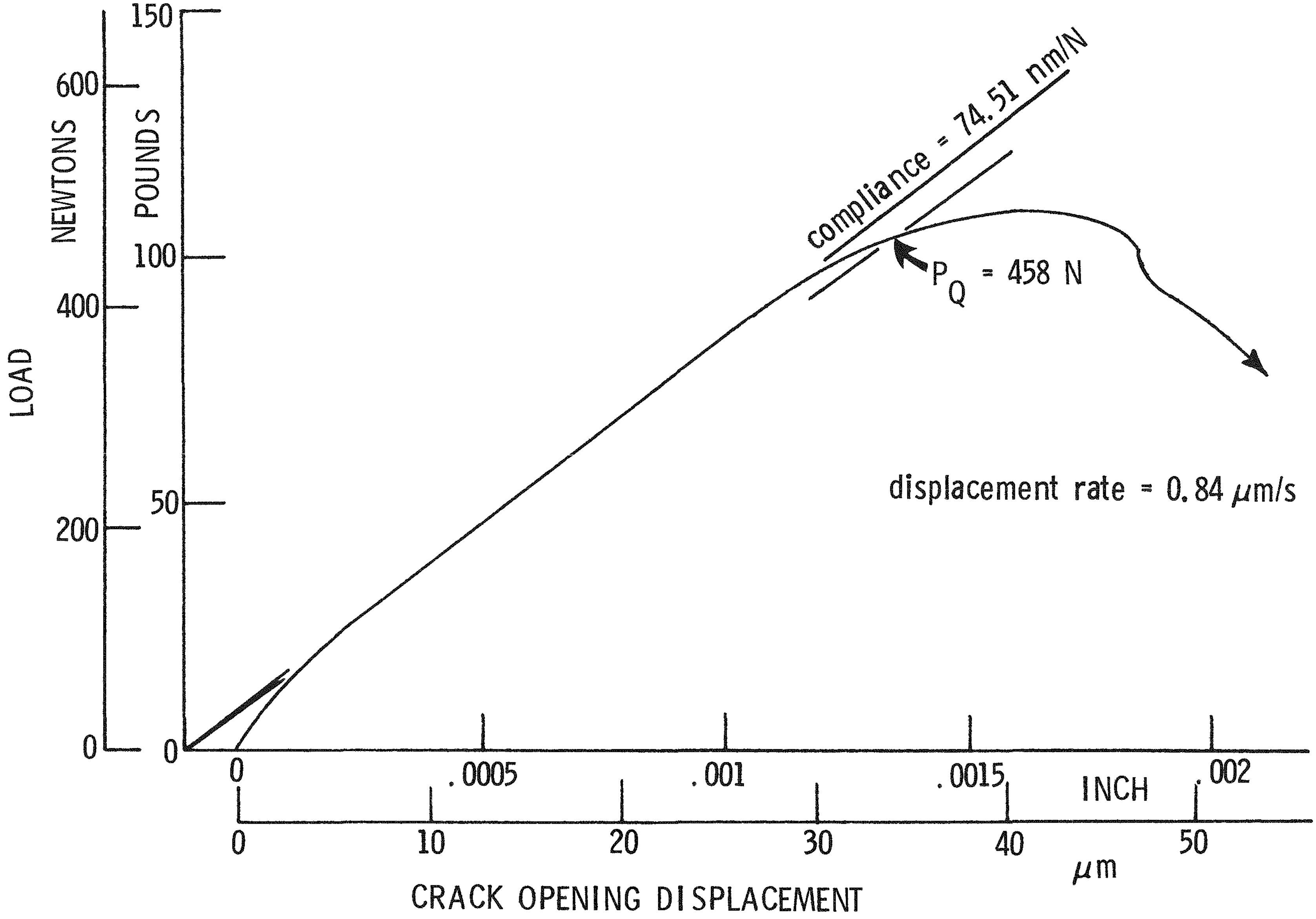

Fig. 7 Load vs. COD for load-to-failure of oil shale fracture specimen.

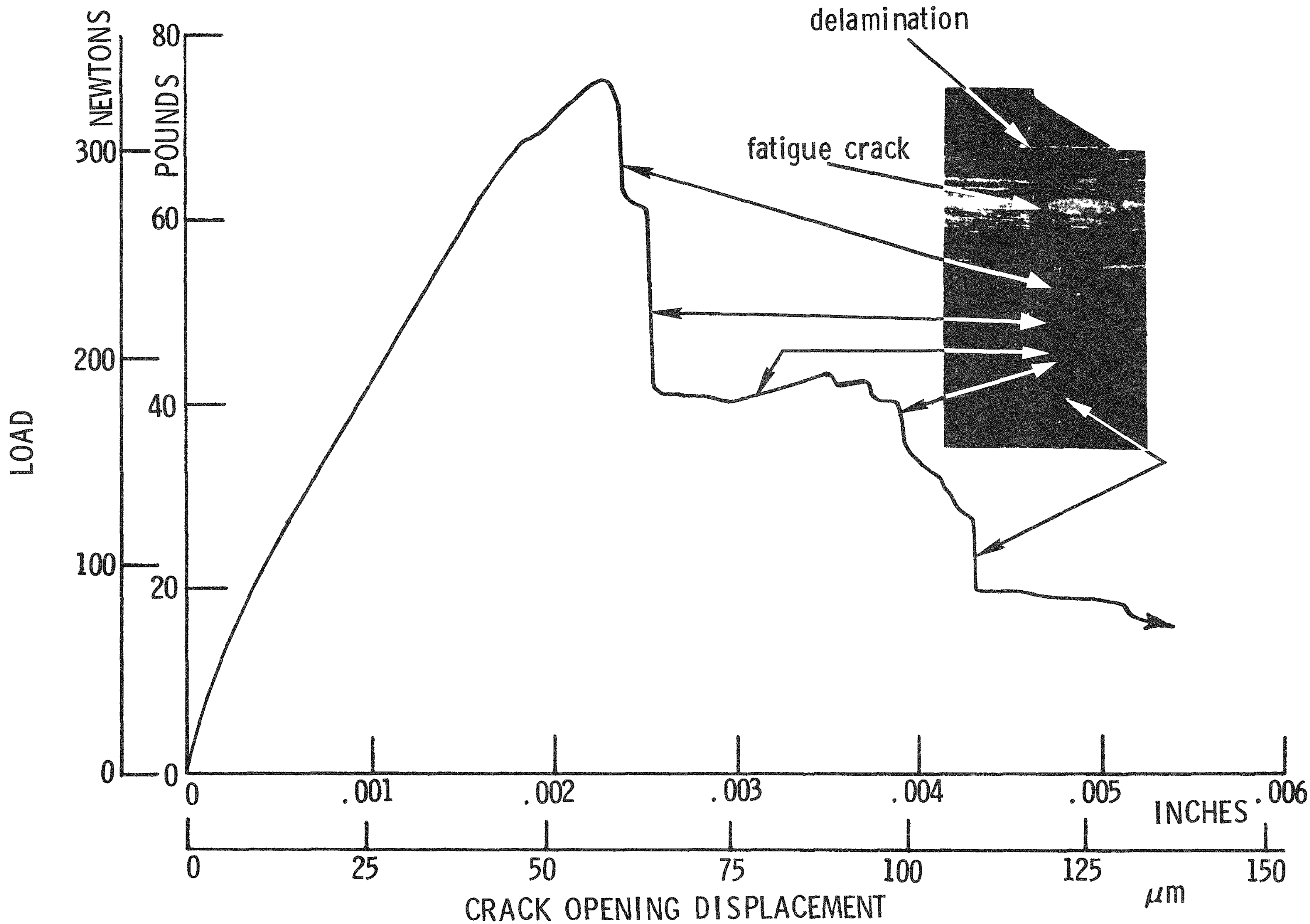

Fig. 8 Load vs. COD for load-to-failure of oil shale fracture specimen tested in arrester geometry. Photo of resulting crack is compared to record showing crack bursts.

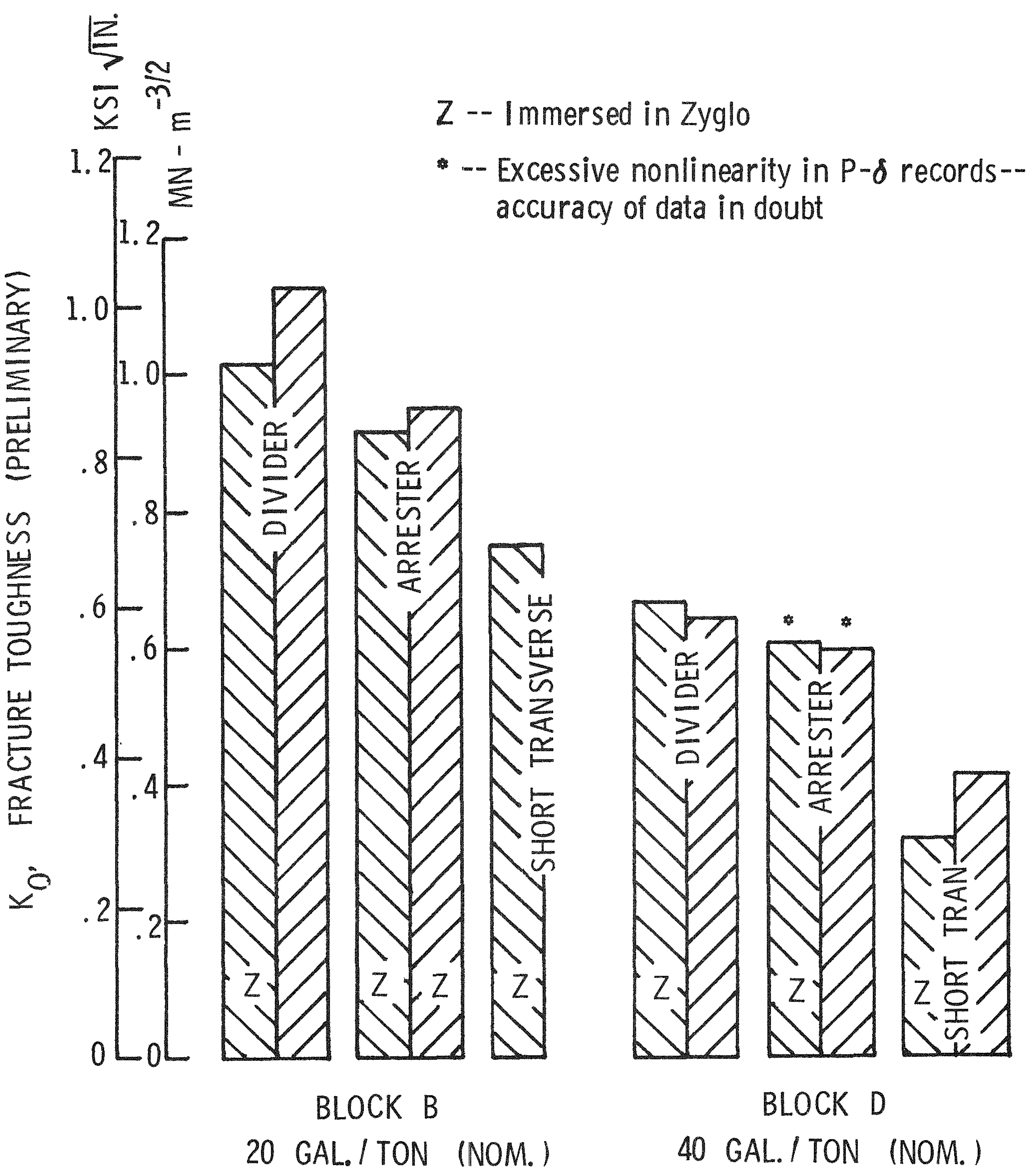

Fig. 9 Preliminary values of fracture toughness for two grades of oil shale tested in the three principal crack orientations.

UNLIMITED DISTRIBUTION

DISTRIBUTION:

U. S. Energy Research and Development Administration
Bethesda Technical Library
Washington, D.C. 20545

U. S. Energy Research and Development Administration
ERDA Library
Washington, D.C. 20545

U. S. Energy Research and Development Administration
Albuquerque Operations Office
P. O. Box 5400
Albuquerque, NM 87115

Dr. Phillip C. White
Asst. Administrator for Fossil Energy
U. S. ERDA
20 Massachusetts Ave. N.W.
Washington, DC 20545

Mr. H. Guthrie
Director
Oil, Gas and Shale Technology
U. S. ERDA/Fossil Energy
20 Massachusetts Ave. N.W.
Washington, DC 20545

Mr. L. M. Burman
Oil, Gas and Shale Technology
U. S. ERDA/Fossil Energy
20 Massachusetts Ave. N.W.
Washington, DC 20545

Mr. H. E. Thomas
U. S. ERDA/Fossil Energy
20 Massachusetts Ave. N.W.
Washington, DC 20545

Harry C. Carpenter
H. B. Jensen
R. L. Wise
Andrew Long
Robert Kerr
R. E. Paulson
Laramie Energy Research Center (6)
U. S. ERDA
Laramie, Wyoming 82070

W. J. Carter, M-6
Los Alamos Scientific Laboratory
Los Alamos, New Mexico 87544

A. E. Lewis
Lawrence Livermore Laboratory
University of California
P. O. Box 808
Livermore, CA 94550

Ahmed S. Abou-Sayed
Terra Tek
University Research Park
420 Wakara Way
Salt Lake City, Utah 84108

Dr. Thomas J. Ahrens
Seismological Laboratory
252-21
California Institute of Technology
Pasadena, CA 91125

Mr. Lynn M. Barker
Terra Tek
420 Wakara Way
Salt Lake City, Utah 84108

Prof. Zdenek P. Bazant
Dept. of Civil Eng.
Northwestern University
Evanston, IL 60201

Dr. William F. Brace
Dept. of Earth and Planetary Science
Mass. Inst. of Technology
Cambridge, MA 02139

Dr. Jim Byerlee
U. S. Geological Survey
Menlo Park, CA 94025

Prof. J. F. Callender
University of New Mexico
Albuquerque, NM 87106

John Ward Smith
Laramie Energy Research Center
U. S. ERDA
Laramie, WY 82070

Ken P. Chong
Associate Professor of Civil Engineering
University of Wyoming
Department of Civil and Architectural Engineering
Laramie, Wyoming 82071

Prof. Rodney J. Clifton
Div. of Engrg.
Brown University
Providence, RI 02912

Dr. Thomas S. Cook
Dept. of Materials Science
Southwest Research Institute
8500 Culebra Road
San Antonio, Texas 78228

Dr. Donald W. Curran
G178
Stanford Research Institute
333 Ravenswood Ave.
Menlo Park, CA 94025

Prof. James W. Dally
Dept. of Mech. Engrg.
University of MD
College Park, MD 20742

Dr. Charles Fairhurst
Dept. of Civil and Mineral Engrg.
Univ. of Minnesota
Minneapolis, MN 55455

Prof. Mel Friedman
College of Geosciences
Center for Tectonophysics
Texas A&M
College Station, TX 77843

G. P. Garrett
Dept of Metallurgy and Materials Science
Univ. of Cape Town
Private Bag, Rondebosch, 7700
Republic of South Africa

Prof. Ken Gray
Dept. of Petroleum Engineering
University of Texas at Austin
Austin, TX 78712

Sidney I. Green
Terra Tek
420 Wakara Way
Salt Lake City, Utah 84108

Dr. John Handin
College of Geosciences
Center for Tectonophysics
Texas A&M
College Station, TX 77843

Michael P. Hardy
Golder and Browner Assoc.
1234 Main Street
Grand Junction, CO 81501

Prof. Dave C. Holloway
Dept. of Mech. Engrg.
Univ. of MD
College Park, MD 20742

Gary Holzhausen
National Center for Earthquake Research
U. S. Geological Survey
Menlo Park, CA 94025

Tony Ingraffea
Dept. of Civil Engrg.
ECOT 4-34
University of CO
Boulder, CO 80302

I. A. Jacobson
Laramie Energy Research Center
P. O. Box 3395
University Station
Laramie, WY 82070

Prof. Hon-Yim Ko
Dept. of Civil Engrg.
University of CO
Boulder, CO 80302

Victor Montenyohl
Dept. of Geology
University of South Carolina
Columbia, SC 29208

Prof. Syd S. Peng
Rock Mechanics and Explosive Research Center - School of Mines
West Virginia University
Morgantown, WV 26506

Jerry Ramsey
U.S. ERDA Fossil Energy
20 Massachusetts Ave. N.W.
Washington, DC 20545

Prof. James R. Rice
Brown University
Providence, RI 02912

Dr. John S. Rinehart
Box 392
Santa Fe, NM 87501

Dr. Fritz Rummel
Ruhr-Universitat Bochum
Institut fur Geophysik
463 Bochum-Querenburg
Postfach 2148
West Germany

Prof. C. J. Schmidt
Geology Dept.
Albion College
Albion, MI

Prof. S. R. Swanson
Mechanical Engineering Dept.
University of Utah
Salt Lake City, Utah

Dr. Mark D. Zoback
U.S. Geological Survey
Menlo Park, CA 94025

1111 L. D. Tyler
5000 A. Narath
Attn: 5200 E. H. Beckner
5400 A. W. Snyder
5700 J. H. Scott
5800 R. S. Claassen
5100 J. K. Galt
Attn: 5110 F. L. Vook
5120 G. J. Simmons
5130 G. A. Samara
5150 J. E. Schirber
5160 W. Herrmann
5162 L. D. Bertholf
5162 M. E. Kipp
5162 W. E. Warren
5163 D. E. Munson
5163 D. E. Grady
5163 K. W. Schuler
5163 R. A. Schmidt (25)
5163 C. W. Huddle
5163 W. R. Wawersik
5166 A. J. Chabai
5167 B. M. Butcher
5730 H. M. Stoller
5735 M. M. Newsom
5734 A. L. Stevens
5835 J. P. Hickerson
8266 Tech. Library (2)
3141 Tech. Library (5)
3151 Tech. Writing (3)
For ERDA/TIC (Unlimited Release)

ERDA/TIC (25)
(3171-1 R. P. Campbell)